MODELING AND NUMERICAL SIMULATION OF SOLAR HYBRID POWER PLANT

Submited on 12/05/2014 – Accepted on 14/12/2014

Abstract

The *aim* of this *paper* is to review and evaluate the performances of a solar tower gas turbine central with a capacity of 11.5 MWe, then we assess the potential to improve the capacity of the installation by adding a combined steam cycle with electrical production equal to 3.5.The numerical study of the installation will be done by calculating the solar fields' effectiveness, and then we simulate the different components of the installation by the TRNSYS 16 software.

The main objective of the study is to give a thermodynamic and economic analysis, and assess the feasibility of the installation for the climatic conditions in Béchar area, located in the south of Algeria.

Keywords: *Solar Gas Turbine, Volumetric Receiver, Combined Rankine Cycle, Energetic and Exergetic Analyses, LEC.*

IMAD EDDINE MERICHE
ABDELHADI BEGHIDJA
KARIMA REZGUI

Laboratory of Renewable Energies and Durable Development, Department of Mechanics, University Constantine 1, Algeria.

I. INTRODUCTION

Solar energy represents an abundant resource and one of the most promising sources of renewable energy, which theoretically could supply the world's energy demand [1].

Currently, there are two approaches for generating electricity from solar energy, the first one is the direct conversion of the solar radiation into electricity (photovoltaic panels), and the second one is the thermal conversion of the solar radiation by concentrating solar power systems (CSP).

The CSP concept is based on concentrating and focusing the direct solar irradiation by mirrors onto the volumetric receiver. The last device transfers thermal energy into conventional power cycles using steam turbines, gas turbines or Sterling engines [2]. Since solar energy is not available 24 hours per day, hybridization of the installation is one of the required solutions if electricity generation at night or during cloudy periods is necessary.

The solar tower power plants employ many sun-tracking mirrors called heliostats to reflect and concentrate the incident sunlight onto a receiver atop the tower; the absorbed solar energy translates into thermal power to generate electricity by Rankine cycle or Brayton cycle.

II. DESCRIPTION OF THE PHYSICAL MODEL

In hybrid solar gas turbine towers, a closed pressurized air receiver absorbs the concentrated solar energy. This energy is used to heat the pressurized air before entering into the combustion chamber of the gas turbine; the heated pressurized air is used to drive a Brayton power cycle [3]. The solar hybrid gas turbine system was tested firstly in the SOLGATE project [4]; and similar projects were tested like the PEGASE hybrid gas turbine system project [5]-[6], which combines a closed solar receiver (REFOS) with a gas turbine.

Our present work seeks a numerical simulation and a thermodynamic study of a high output solar gas turbine tower plant with a combined steam cycle as an additional component, which will recover the latent heat of fume exhausted to drive the Rankine steam cycle as presented in figure 1 and figure 2.

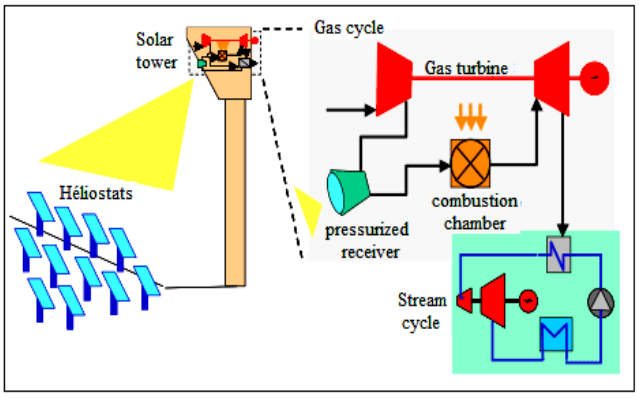

Fig.1. Combined solar gas turbine installation [5]

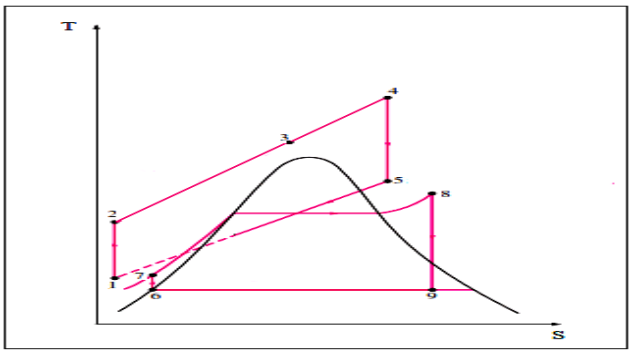

Fig.2. (T–S) Diagrams of the combined installations

III. SOLAR ENERGY POTENTIAL IN ALGERIA

Algeria is characterized by abundant sunshine throughout the year, low humidity and precipitation, and plenty of unused flat land especially in the Sahara region (1.787.000 km^2).

Algeria is counted as one of the sunniest countries in the world, with duration of sunshine up to 3500 hours/year, and the average energy received on a horizontal surface is equal to 1700 kWh/m^2/year on the North of the country, and 2263 (kWh /m2 / year) in the desert and south of it [7].

According to the study of the German Aerospace Centre, Algeria has the largest long term land potential for concentrating solar thermal power plants (CSP) [8]-[9].

IV. MATHEMATICAL FORMULATION

A. Energy balance

The energy balances of the different components in the solar gas turbine system are [10]:

- *Air compressor*

The air *compressor* input power [13] is found as:

$$\dot{W}_C = \dot{m}_a Cp_a (T_2 - T_1) \quad (1)$$

$$T2 = T_1 \left(1 + \frac{1}{\eta_{AC}} \left(r_{AC}^{\frac{\gamma_a - 1}{\gamma_a}} - 1\right)\right)$$

$$Cp_a(T) = 1.048 - \left(\frac{3.83\,T}{10^4}\right) + \left(\frac{9.45T^2}{10^7}\right) - \left(\frac{5.49T^3}{10^{10}}\right) + \left(\frac{7.92T^4}{10^{14}}\right)$$

- *Solar receiver*

The sunlight solar flux I_c is reflected by a surface S_c of the heliostat field and intercepted by the volumetric solar receiver.The thermal power intercepted in the cavity of the closed volumetric receiver is written [11] :

$$\dot{Q}_C = \eta_{field}\, I_c S_c \quad (2)$$

The matrix of the solar effectiveness field η_{field} includes the reflectivity of the mirror (ρ_{Mirr}), the cosine effect (η_{cos}), the shades effect and blockings ($\eta_{Block,shad}$), the atmospheric effect (η_{Atmos}), and the interception effect (η_{Int}) [12, 13] (figure 3) is written as:

$$\eta_{field} = \rho_{\text{Mirr}} \times \eta_{cos} \times \eta_{Block,shad} \times \eta_{Atmos} \times \eta_{\text{Int}} \quad (3)$$

With:

$$\begin{cases} \eta_{cos} = \frac{\sqrt{2}}{2}\left[\sin(\alpha)\cos(\lambda) - \cos(\theta_H - A)\cos(\alpha)\sin(\lambda) + 1\right]^{0.5} \\ \eta_{Atmos} = \begin{cases} 0.99321 - 0.000176\, S_0 + 1.97\, 10^{-8} S_0^2 \\ \exp(-0.0001106\, S_0) \end{cases} ;\ S_0 \geq 1000m \\ \eta_{intercept} = \frac{1}{2\pi\, \sigma_{tot}^2} \int(x) \int(y) \exp\left(\frac{-x^2+y^2}{2\,\sigma_{tot}^2}\right) dxdy \\ \sigma_{tot} = (\sigma_{solar}^2 + \sigma_{mirror}^2 + (2\,\sigma_{track})^2)^{0.5} \end{cases}$$

$\eta_{Block,shad}$: The value is obtained by the positioning of heliostats field (HFLD code) [13].

Numbers of commercial software packages are used to optimize the heliostats field as: HELIOS, DELSOL, HFFCAL, SOLERGY, and SOLTRACE [5]

The closed volumetric receiver (REFOS) uses air as a working fluid.

The thermal power transmitted between the interior cavities of the receiver and the pressurized air loses a fraction of energy by reflection, natural convection and radiation. [13]

The transmitted power in the receiver is:

$$\dot{Q}_r = \dot{Q}_C - h_{cv} A_r (T_r - T_0) - \sigma\, \varepsilon\, A_r (T_r{}^4 - T_0{}^4) \quad (4)$$

$$\dot{Q}_r = \dot{m}_{air} Cp (T_3 - T_2) \quad (5)$$

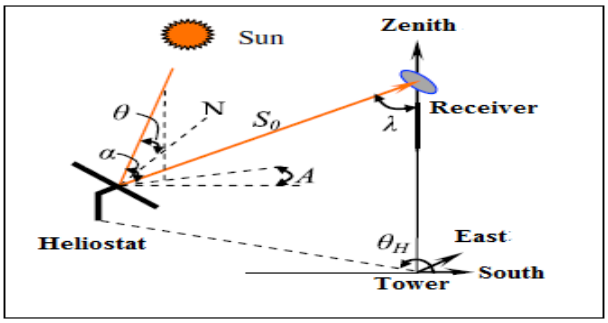

Fig.3. Angles and position of the heliostat relative to the receiver [13]

- Combustion chamber

In the combustion chamber, the natural gas is injected and burned with the pressurized air [14].

$$C_n H_m + A\left(\frac{n+m}{4}\right).[O_2 + 3.76\, N_2] \rightarrow (n) CO_2 + \left(\frac{m}{2}\right) H_2O + \left[(A-1).\left(n + \frac{m}{4}\right)\right] O_2 + \left[3.76A\left(\frac{n+m}{4}\right)\right] N_2$$

The output properties of the combustion chamber vary depending on the mass flow rate of the air, the fuel lower heating value (LHV) and the combustion efficiency.

$$\dot{m}_a h_3 + \dot{m}_f . LHV = \dot{m}_g h_4 + (1 - \eta_{cc}) \dot{m}_f . LHV \quad (6)$$

- Turbine

The expansion in the turbine produces the mechanical power required to drive the compressor and the electrical generator.The power produced by the turbine is given by :

$$\dot{W}_T = \dot{m}_g Cp_g (T_4 - T_5) \quad (7)$$

With : $\dot{m}_g = \dot{m}_f + \dot{m}_a \quad (8)$

$$Cp_g(T) = 0.991 + \left(\frac{6.997\,T}{10^5}\right) + \left(\frac{2.712\,T^2}{10^7}\right) - \left(\frac{1.224\,T^3}{10^5}\right) \quad (9)$$

- Alternator

The alternator is a rotating electromagnetic machine that converts the mechanical energy produced by the turbine into electrical energy with efficiencies between: 85% to 95%.

The electric output power is also found as:

$$P_{ele} = W_{GT} . \eta_{al} \quad (10)$$

The energy balances of the different components [15] of the steam cycle are:

- Pump

The work provided by the pump is expressed as follows:

$$W_p = \frac{\dot{m}_6 (h_7 - h_6)}{\eta_p} \quad (11)$$

- Steam generator

The exhaust gases of the gas turbine are transferred to the heat recovery steam generator (HRSG), which comprises the economizer, evaporator and super heater. In the steam generator, the contribution of energy to the steam is:

$$Q_{SG} = \dot{m}_7 (h_8 - h_7) \quad (12)$$

- Steam turbine

The work provided by the turbine is expressed as:

$$W_{ST} = \dot{m}_8\, \eta_{st} (h_9 - h_8) \quad (13)$$

- Condenser

The thermal power rejected into the condenser is expressed by:

$$Q_{cond} = \dot{m}_9 \, (h_6 - h_9) \quad (14)$$

B. Exergy balance

Exergy analysis can evaluate and indicate the causes of the thermodynamic imperfection in the energy system [16].

The exergy is defined as the maximum useful work that can be done by a system interacting with a reference environment and it is divided into physical and chemical exergy. By applying the second law of thermodynamics we obtain the exergy balance:

$$\dot{E}x_Q + \sum_i \dot{m}_i ex_i = \sum_e \dot{m}_e ex_e + \dot{E}x_W + \dot{E}x_D \quad (15)$$

With:

$$\dot{E}x_Q = (1 - \frac{T_0}{T_i})\dot{Q}_i \quad (16)$$

$$\dot{E}x_W = \dot{W} \quad (17)$$

$$ex = ex_{ph} + ex_{ch}$$

$$ex_{ph} = (h - h_0) - T_0(s - s_0) \quad (18)$$

The chemical exergy of the gas mixture is defined as follows:

$$ex_{ch}^{mix} = [\sum_{i=1}^{n} x_i ex^{ch_i} + RT_0 \sum_{i=1}^{n} x_i \ln x_i \,] \quad (19)$$

$\dot{E}x_Q$,$\dot{E}x_W$: Thermal exergy and power exergy.

ex_{ph}, ex_{ch}: Physical exergy and chemical exergy.

- Heliostats fields

Exergy expression of heliostat field [17] is given as:

$$Ex_{hel} = Ex_{rec} + Ex_{hel,loss} \quad (20)$$

$$Ex_{hel} = \dot{Q_{hel}}(1 - \frac{T_0}{T_{sol}}) \quad (21)$$

$$Ex_{rec} = \dot{Q_r}(1 - \frac{T_0}{T_{sol}}) \quad (22)$$

Exergy efficacy of heliostats field is:

$$\eta_{ex,hel} = \frac{Ex_{rec}}{Ex_{hel}} \quad (23)$$

- Volumetric receiver

The exergy expression in the solar receiver [17] is given as:

$$Ex_{rec} = Ex_{rec,abs} + Ex_{rec,loss} + IR_{rec} \quad (24)$$

$$Ex_{rec,loss} = \dot{Q}_{rec,tot\,loss}(1 - \frac{T_0}{T_{rec}}) \quad (25)$$

$$Ex_{rec,abs} = m\,[(h_3 + h_2) - T_0(s_3 - s_2)] \quad (26)$$

Exergy efficacy of the solar receiver is:

$$\eta_{ex,rec} = \frac{Ex_{rec,abs}}{Ex_{rec}} \quad (27)$$

The expression of exergetic efficiencies of the gas turbine components [18] are in table 1.

Components	Destruction of Exergy	Exergy Efficiencies
Compressor	$\dot{E}x_{D,AC} = \dot{E}x_1 - \dot{E}x_2 + \dot{W}_{AC}$	$\eta_{ex,AC} = \frac{\dot{E}x_2 - \dot{E}x_1}{\dot{W}_{AC}}$
Combustion chamber	$\dot{E}x_{D,cc} = \dot{E}x_3 + \dot{E}x_f - \dot{E}x_4$	$\eta_{ex,CC} = \frac{\dot{E}x_4}{\dot{E}x_3 + \dot{E}x_f}$
Turbine	$\dot{E}x_{D,GT} = \dot{E}x_5 - \dot{E}x_4 + \dot{W}_{GT}$	$\eta_{ex\,GT} = \frac{\dot{W}_{GT}}{\dot{E}x_4 - \dot{E}x_5}$

The expressions of exergetic efficiencies in the various components of the steam turbine [17]-[18] are in table 2.

TABLE II. EXERGETIC EFFICIENCIES OF THE STREAM CYCLE

Components	Exergy Destruction	Exergy Efficiencies
Pump	$\dot{E}x_{D,P} = \dot{E}x_7 - \dot{E}x_6 + \dot{W}_P$	$\eta_{ex,P} = \frac{\dot{E}x_7 - \dot{E}x_6}{\dot{W}_P}$
Steam generator	$\dot{E}x_{D,SG} = \dot{E}x_{IN} - \dot{E}x_{OUT}$	$\eta_{ex,SG} = \frac{\dot{E}x_8 - \dot{E}x_7}{\dot{E}x_5 - \dot{E}x_6}$
Turbine	$\dot{E}x_{D,Tv} = \dot{E}x_8 - \dot{E}x_9$	$\eta_{ex\,Tv} = \frac{\dot{W}_{Tv}}{\dot{E}x_8 - \dot{E}x_9}$
Condenser	$\dot{E}x_{D,cond} = \dot{E}x_{IN} - \dot{E}x_{OUT}$	$\eta_{ex,Cond} = 1 - \frac{\dot{E}x_{D,cond}}{\dot{E}x_{IN}}$

V. SIMULATION OF INSTALLATION AND PARAMETERS

A. Simulation

The radiation view factor was calculated by an algorithm which develops a Monte-Carlo ray-tracing technique.The algorithm calculates the vector leaving the originating surface at a random location, angle, elevation, and checks if the vector intersects the polygon on the target surface [19].The Monte-Carlo ray tracing algorithm [19] was applied and inserted in the TRNSYS model [20].

The simulation and the design of the optics and the thermal model parts of the solar gas turbine with combined cycle was optimized using TRNSYS 16 software including STEC 3.0 library (Solar Thermal Electric Components) [20] figure 4, the inputs parameters in the simulation are the hourly solar irradiance, meteorological data, site information and technical system data.

To validate the numerical model simulated in TRNSYS software of the solar gas turbine, we use the numerical study of the solar gas turbine PGT10 (simulated with TRNSYS16) verified in the SOLGATE project as a reference [4], than we calibrated our solar gas turbine model by the different parameters data provided by the manufacturer [21]. The numerical model of steam turbine has been elaborated and validated by an existing steam turbine power plant.

B. Parameters of the installation

The solar gas turbine with combined cycle are considered to be operating at its nominal point, the gas turbine, steam turbine, compressor and pump units have been characterised by their isentropic efficiencies [21]-[22]. All parameters of the solar gas turbine and steam cycle are given in table 3 and table 4.

TABLE I. EXERGETIC EFFICIENCIES OF THE GAS TURBINE

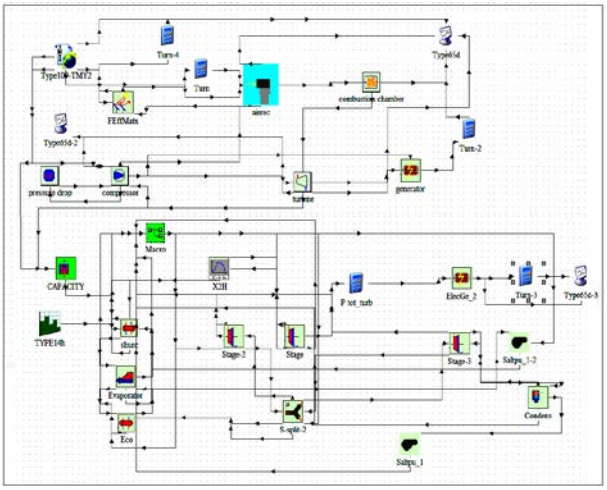

Fig.4. Simulation of the combined installations in TRNSYS16 software

TABLE III. PARAMETERS OF THE INSTALLATION

Parameters	Value
Brayton Cycle	
Output temperature of combustion chamber	1000 °C
Calorific value of natural gas in Algeria (**LHV**)	45119 kJ/kg
Compressor isentropic efficiency	86 %
Atmospheric conditions	100 kPa, 25°C
Turbine isentropic efficiency	85 %
Chamber combustion efficiency	95 %
Electromechanical efficiency of generator	98 %
Pressure lost in the solar receiver	1,25 %
Pressure lost in the combustion chamber	4 %
Compressor pressure	11.1 bar
Air mass flow used (**ṁ**)	56.2 Kg/s
Pressure of exhaust fumes	101.5 KPa
Rankine Cycle	
Steam pressure	58.4 bar
Steam mass flow	3.7 Kg/s
Condensation pressure	0.13 bar
Condensation temperature	45.1°C
Turbine isentropic efficiency	90 %
Pump isentropic efficiency	90 %

TABLE IV. PARAMETERS OF THE SOLAR TOWER CONCENTRATOR [4]

Parameters	Value
Reflectivity of mirrors	92 %
Total error (σ_{tot})	4 mrad
Receiver area	52 m^2
Heliostat reflective area	11×11 m^2
Average direct normal irradiation (I)	800 W/m^2

VI. PERFORMANCE OF THE INSTALLATION

To calculate the daily performances of the installation we selected the average solar irradiation profiles of Béchar area.

The average efficiencies of the solar field calculated by FORTRAN code [19] and verified by the software SolTrace [4] are given in Table 5.

TABLE V. SOLAR FIELD EFFICIENCIES

ρ_{Mirror}	η_{cos}	$\eta_{Block,shad}$	η_{Atmos}	$\eta_{intercept}$
88 %	89.60 %	94.45 %	96.32 %	99.47

A. Influence of direct normal solar irradiation on the absorbed solar energy and consumption of natural gas:

Direct normal solar irradiation (DNI) has a direct impact on the absorbed solar energy in the receiver and consumption of natural gas in the combustion chamber.

In figure 5 we can see, that the absorbed solar energy in the receiver increases with the direct normal solar irradiation, which implies the decrease of natural gas fuel consumption in the combustion chamber.

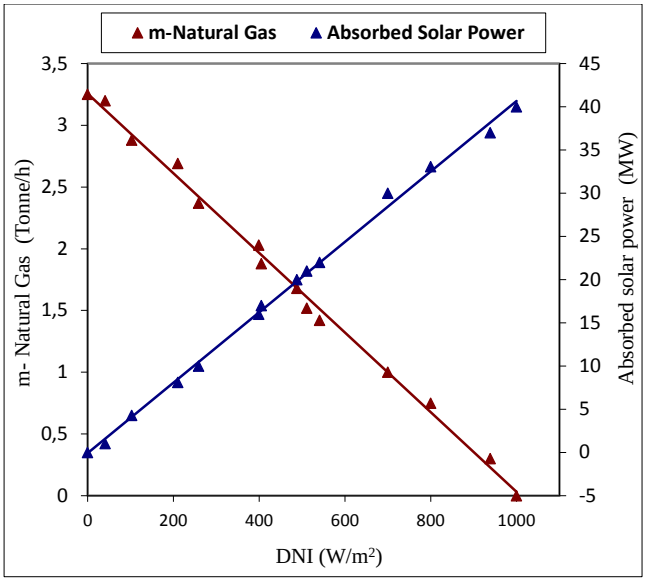

Fig.5. Variation of natural gas consumption and absorbed solar energy according to direct solar irradiation

B. Energy efficiencies

To calculate the energetic performances of the solar gas turbine without and with the combined steam cycle, we take the optimal conditions of solar irradiation and the best performances of the heliostats fields obtained by a typical clear day, the results are given in table 6.

TABLE VI. ENERGY EFFICIENCIES OF THE INSTALLATION

Subset	Energy (M Watt)	Temperature (°C)	Efficiency (%)
Heliostat field	P_{sol} = 58.98	T_{amb} =20	71.35
Receiver	$\dot{Q_C}$ = 42.08 $\dot{Q_r}$ = 33.09	T_2 = 363 T_3 = 845	78.63
Gas Turbine	P_{fuel} = 13.54 $\dot{W_{GT}}$ =11.73	T_4 = 1000 T_5 = 425	-
Brayton Cycle	P_{elec} = 11.5	-	20.67
Rankine Cycle	P_{elec} = 3.5	T_7 = 51.25 T_8 = 345	32.31
Combined Cycle	P_{el}= 15	-	26.96

C. Exergy efficiencies

After calculating the energetic efficiencies, we calculate the exergy efficiencies of the solar installation with the combined steam cycle, the results are represented in figure 6.

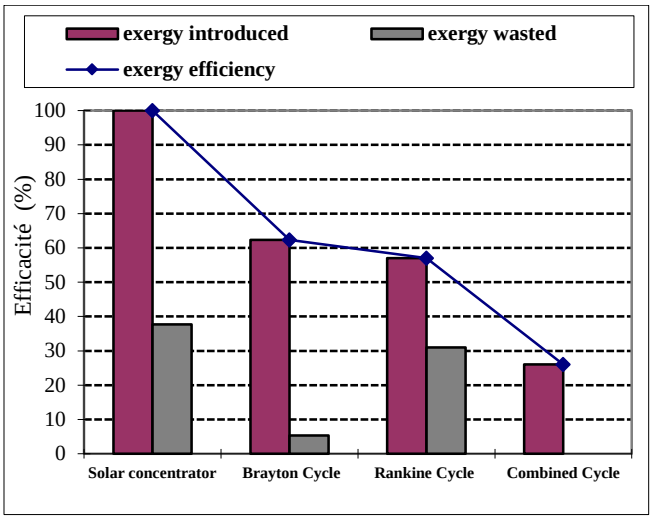

Fig.6. Exergy efficiencies of the installation

VII. DAILY PERFORMANCES

The plant is considered to be located in Southern Algeria region of Béchar (figure 7), solar irradiation and climatic conditions data has been obtained for the generic day (21/03/2010), shown in figure 8, this date is chosen in order to avoid under sizing of the heliostats field area [23].

Fig.7. Geographic location of Béchar area

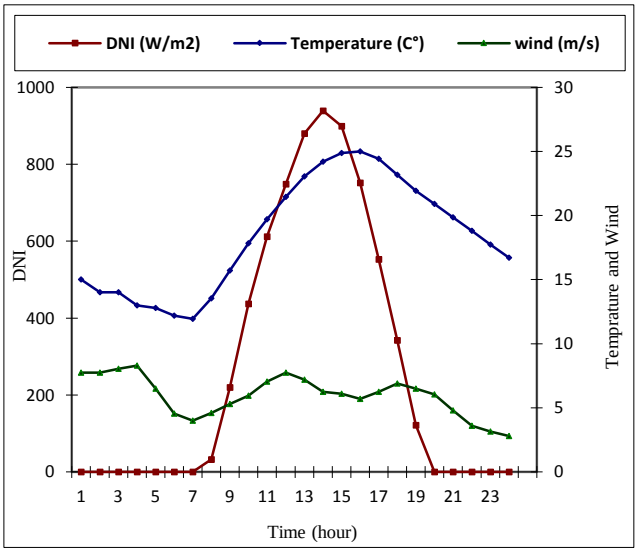

Fig.8. Daily variation of temperature, wind and solar irradiation in Béchar area (21 Mars 2010)

Using daily variation in figure 8, we calculate the temporal evolution of absorbed and received solar power, electrical production and fuel power consumption in the combined installation; the results are given in figure 9.

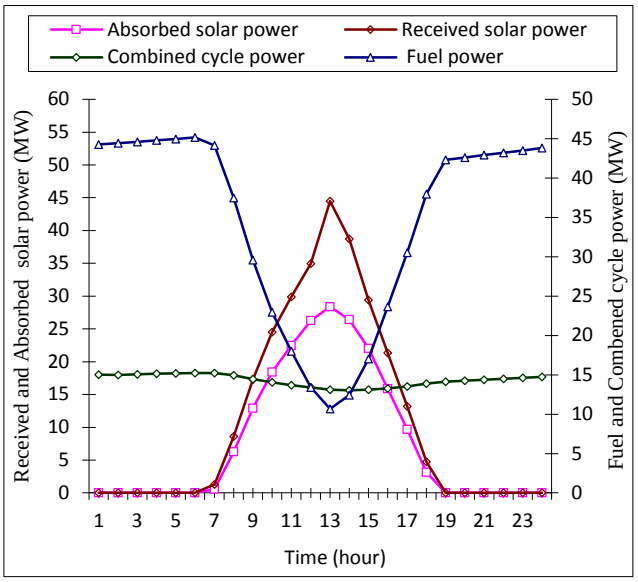

Fig.9. Temporal evolution of the powers in the installation (21 mars 2010)

A. Energetic and exergetic daily efficiencies performances

With the daily variation of energies represented in figure 9, we calculate the temporal evolution of energetic and exergetic efficiencies in the solar gas turbine installation without and with the combined steam cycle; the results are represented in figure 10 and figure 11.

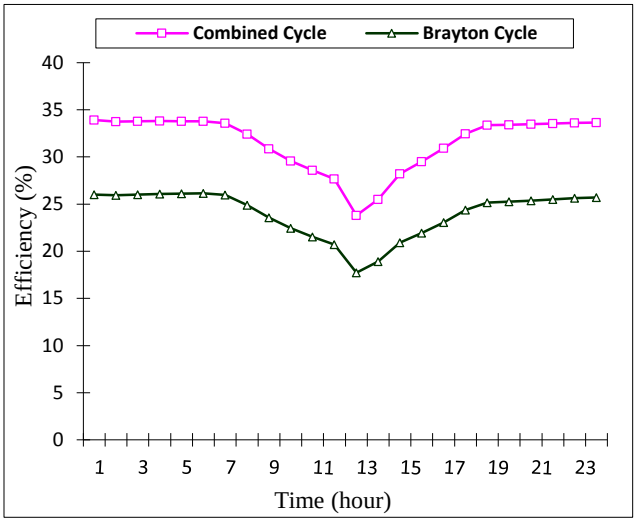

Fig.10. Temporal evolution of energetic efficiencies in the solar installation

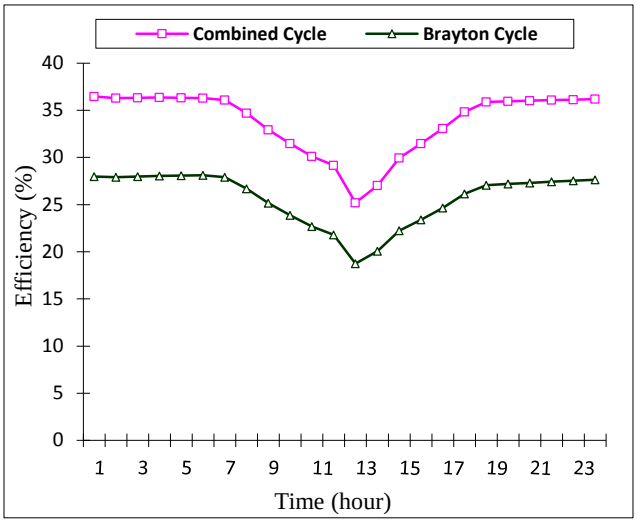

Fig.11. Temporal evolution of exergetic efficiencies in the solar installation

VIII. ECONOMIC ANALYSIS OF THE INSTALLATION

The economic analysis is done by an estimation of the Levelized electric cost of the combined solar-gas turbine. With data taken from the ECOSTAR report [24] and the other original works as Lovegrove [25], Frangopoulos [26], and Spelling [22], we calculate the installation total investment cost (Table 7).

The levelized electric cost (LEC) [27] is expressed as follows:

$$LEC = \frac{f.C_{inv}+C_{O\&M}+C_{fuel}}{E_{net}} \quad (28)$$

With:

$$f = \frac{k_d(1+k_d)^n}{(1+k_d)^n-1} + k_{insurance} \quad (29)$$

$$C_{O\&M} = 9.36\ (A_{helio}\ .N_{helio}) \quad (30)$$

Using the energetic performance results, we calculate the annual electricity production and the annual fuel consumption in the installation.

The levelized electric cost of the combined solar gas turbine power plant is shown in Table 8.

TABLE VII. COMPONENT'S COSTS OF THE COMBINED SOLAR-GAS TURBINE

Component	Cost	
Gas Turbine System	7'159'000	[USD]
Steam turbine system	3'595'000	[USD]
Waste heat boiler	2'271'000	[USD]
Air-cooled condenser	6'950'000	[USD]
Feedwater pump	14'000	[USD]
Central tower	2657000	[USD]
Volumetric receiver	1183000 (52 m^2)	[USD]
Heliostat field	9279400 (585 Heliostat)	[USD]
Power electronics and control	2'435'000	[USD]
Civil engineering works	14'545'000	[USD]
Total Investment Cost	50088400	[USD]

TABLE VII. LEVELIZED ELECTRIC COST OF THE COMBINED SOLAR-GAS TURBINE POWER PLANT

Result	Value	
Total installation investment cost (C_{inv})	5008840 0	[USD]
depreciation period (n)	25	[yrs]
Real interest rate (k_d)	8	[%]
Annual insurance rate($k_{insurance}$)	1	[%]
Annual electricity production (E_{net})	125.6	[GWh]
Annual fuel cost (C_{fuel})	1050800	[USD]
Operation and maintenance costs ($C_{O\&M}$)	657072	[USD]
Levelized Electrical Cost (LEC)	0.0549	[USD/kWhe]

IX. DISCUSSION OF RESULTS

The energy analysis results represented in table 6 shows a clear improvement in the energetic performances of the solar gas turbine by using a combined cycle; we note an increase in the electrical power production up to 15 MWe, and a gain of 6,29 % in the energetic efficiency.

The exergy analysis results obtained in Figure 6 reveals that the exergy destruction in the solar gas turbine installation is caused mostly in the solar receiver and combustion chamber. After calculating the daily performances of the installation as shown in figures 9, we note that the crossing in the absorbed solar energy causes a reduction of the electrical power production. This reduction is explained by a diminution of the consumption of the natural gas inside gas turbine as verified in figure 5, and the high ambient temperatures amplify these reductions.

The decreasing of the ambient temperature especially in night hours generates an improvement on the electrical power production and increases the energetic efficiencies, the results in figure 10 and figure 11 shows a sharp improvement in the energetic and exergetic performances of the installation by using a combined cycle.

Finally, by the economic analysis of the power plant in Table 8, we note that the annual consumption cost of fuel gas remains one of the major factors which influence the levelized electric cost LEC.

CONCLUSION

In this research paper, a preliminary evaluation and simulation of a solar gas turbine installation have been made with an electric power production equal to 11.5 MWe. Then we study the potential improvement of this installation by introducing a combined steam cycle, which uses the latent heat of the exhaust gases as a source of energy with an electrical production equal to 3.5 MWe.

By using the thermodynamic study, we note that the most important causes of the efficiencies decreases of the installation are related to the loss of combustion energy evacuated by the exhaust gases of the solar gas turbine. Moreover, the use of a combined steam cycle is the best solution to decrease the exergetic irreversibility of the installation and increase the energetic and exergetic efficiencies (a gain of 5.19 % in the exergetic efficiency).

With LEC = 52 USD/MWe, (one of the lowest LEC of concentrating solar power plants), the economic study proves the promising potential of the combined solar gas turbine installation , especially in south Algeria such as Béchar area.

NOMENCLATURE

Q_r : Power transmitted by the cavity of the receiver (Watt)
Q_c: Power received in the cavity of receiver (Watt)
Cp: Specific heat (kJ / kg K)
A_r : Receiver area (m^2)
I_c : The direct incident solar power (W/m^2)
S_c : The sensor surface of heliostats fields (m^2)
T_0: Ambient temperature (°C)
T_r : Temperature in the receiver (°C)
h_{cv}: Heat transfer coefficient (W/m^2K)
ṁ : Mass flow (Kg/s)
LHV: Lower calorific values of natural gas (KJ/Kg)
LEC: Levelized Electric Cost (USD/MWe)
$\dot{W}_{GT}$: Gas Turbine power (Watt)
$\dot{W}_C$: Compressor power (Watt)
P_{solar} : Solar power transmitted by heliostats (Watt)
P_{rec} : Solar power received (Watt)
$Q_{rec,tot\ loss}$: Total energy losses in receiver (Watt)
Ex_{rec} : Exergy in the receiver (Watt)
$Ex_{rec,loss}$: Exergy losses in the solar receiver (Watt)
$Ex_{rec,abs}$: Exergy absorbed by the solar receiver (Watt)
IR_{rec} : Irrevercibity power in the solar receiver (Watt)
$\dot{m}_f$: Mass flow of the natural gas used in combustion (Kg/h)
$\dot{m}_a$: Mass flow of air (Kg/h)
$\dot{m}_g$: Mass flow of gases (Kg/h)
Cp_g : Specific heat of gases (kJ / kg K)
$Ex_{rec,loss}$: Exergy losses in the receiver (Watt)
$\dot{E}x_f$: Exergy of the fuel gas (Watt)
Ex_{sol} : Solar exergy (Watt)
$\dot{E}x_{D,rec}$: Destruction exergy in the receiver (Watt)
$\dot{E}x_{D,GT}$: Destruction exergy in solar gas turbine cycle (Watt)
$Ex_{D,Ran}$: Destruction exergy in Rankine cycle (Watt)
η : Efficiency
η_{st} : Efficiency of steam turbine
ε : Absorber Emissivity.
σ : Stefan Boltzmann constant ($5{,}670 \times 10^{-8} W/m^2.K^4$)
$\eta_{ex.hel}$: Exergy efficiency of heliostats
$\eta_{ex\ D,rec}$: Efficiency of destruction exergy in receiver
$\eta_{ex\ D,GT}$: Efficiency of destruction exergy in solar gas turbine
$\eta_{ex,inst}$: Exergy efficiency of combined cycle
$\eta_{ex\ D,Ran}$: Efficiency of destruction exergy in Rankine cycle

REFERENCES

[1] A. Ferrière. “Centrales solaires thermodynamiques. Edition Techniques de l’Ingénieur”, BE 8 903, pp 1-20, 2007.

[2] S.Bonnet, M. Alaphilippe, P. Stouffs. “Thermodynamic solar energy conversion: Reflections on the optimal solar concentration ratio”. International Journal of Energy, Environment and Economics,vol12, pp141-152., 2006.

[3] G. Barigozzi, G. Bonetti, G. Franchini, A. Perdichizzi, S. Ravelli. “Thermal performance prediction of a solar hybrid gas turbine. Solar Energy”, vol 86, pp2116–2127, 2012.

[4] European Commission. SOLGATE Solar hybrid gas turbine electric power system – final publishable report, 2002. http://ec.europa.eu/ research/energy/pdf /solgate.

[5] Pirre Garcia, Alain Ferrier, G. Flamant, P. Costerg et al. “Solar field efficiency and electricity generation estimations for a hybrid solar gas turbine project in France”. Journal of Solar Energy Engineering, vol 130, pp 145021-145023, 2008.

[6] Peter Schwarzbözl, M .Schmitz, R .Pitz-Paal, R. Buck. Analysis of “Solar Gas Turbine Systems with Pressurized Air Receivers (REFOS)”, 11th International Symposium on Concentrated Solar Power and Chemical Energy Technologies. Zürich, Switzerland, September 4-6, 2002.

[7] A. Boudghene Stambouli, Z.Khiat, S.Flazi, Y.Kitamura. “A review on the renewable energy development in Algeria: Current perspective, energy scenario and sustainability issues”. Renewable and Sustainable Energy Reviews, vol 16, pp 4445–4460, 2012.

[8] Michael Geyer. START Mission to Algeria edited by IEA. Report on the Solar PACES; Start Report September 2003.

[9] F. Trieb, C. Schillings, M. O’Sullivan, T. Pregger, C. Hoyer-Klick. Global potential of concentrating solar power. German Aerospace Centre (DLR) 2009.

[10] G. Barigozzi, G. Bonetti, G. Franchini, A. Perdichizzi, S. Ravelli. “Thermal performance prediction of a solar hybrid gas turbine”. Solar Energy, 86, pp 2116–2127, 2012.

[11] Robert Pitz-Paal, Nicolas Bayer Botero, Aldo Steinfeld. “Heliostat field layout optimization for high-temperature solar thermo-chemical processing”. Solar Energy, vol 85; pp 334–343, 2011.

[12] Pierre Garcia, Alain Ferriere, Jean-Jacques Bezian. “Codes for solar flux calculation dedicated to central receiver system applications”. Solar Energy, vol 82, pp 189–197, 2008.

[13] Xiudong Wei, Zhenwu Lu, “A new method for the design of the heliostat field layout for solar tower power plan”t. Renewable Energy, vol 35, pp 1970–1975, 2010.

[14] Matthias russ. Elaboration of thermo-economic models of solar-turbine power plants. Master thesis. Institut für thermische Strömungsmaschinen, May 2011.

[15] John. A. Duffie and William. A. Beckman. Solar engineering of thermal processes, 2nd edition, New York: Wiley (1991).

[16] Chao Xu, Zhifeng Wang, Xin Li, Feihu Sun. "Energy and exergy analysis of solar power tower plants". Applied Thermal Engineering, vol 31, pp 3904-3913, 2011.

[17] Pouria Ahmadi, Ibrahim Dincer, Marc A. Rosen. "Exergy, exergo-economic and environmental analyses and evolutionary algorithm based multi-objective optimization of combined cycle power plants". Energy, vol 36, pp 5886-5898, 2011.

[18] V. Siva Reddy, S.C. Kaushik, S.K. Tyagi. "Exergetic analysis of solar concentrator aided natural gas fired combined cycle power plant". Renewable Energy, vol 39, pp114-125, 2012.

[19] Lukas Feierabend, Thermal model development and simulation of cavity-type solar central receiver systems. Master These. University of Wisconsin Madison, United States., 2009.

[20] TRNSYS16 Tutorial & application; operation guides. TRNSYS STEC 3.0 and TESS available from: http://sel.me.wisc.edu /trnsys/trnlib/ tees/stec.htm.

[21] GE Energy, Gas Turbine Performances Data, 2007.

[22] James Spelling, Thermo-Economic Optimisation of Solar Tower Thermal Power Plants, Ecole Polytechnique Fédérale de Lausanne, Master Thesis 2009

[23] Climatic Condition METEONORM V 7.0.

[24] R. Pitz-Paal, J. Dersch, B. Milow , European Concentrated Solar Thermal Road-Mapping (ECOSTAR), Deutsches Zentrum für Luftund Raumfahrt, Köln, 2004.

[25] K. Lovegrove, W. Stein, Concentrating Solar Power Technology: Principles, Developments and Applications, Woodhead Publishing,Cambridge, 2012.

[26] C.FRANGOPOULOS, "Introduction to Environomics" ASME, AES, vol 191, pp 49-54, 1991.

[27] Peter Schwarzbözl, Reiner Buck, " Chemi Sugarmen. Solar gas turbine systems: Design, cost and perspectives". Solar Energy, vol80, pp1231–1240, 2006.